# Impact of Geophysical and Datum Corrections on Absolute Sea-Level Trends from Tide Gauges around Taiwan, 1993–2015

**Wen-Hau Lan [1],\*** [iD]**, Chung-Yen Kuo [1]** [iD]**, Huan-Chin Kao [1], Li-Ching Lin [2], C. K. Shum [3,4]** [iD]**, Kuo-Hsin Tseng [5]** [iD] **and Jung-Chieh Chang [6]**

[1]  Department of Geomatics, National Cheng Kung University, Tainan 70101, Taiwan;
    kuo70@mail.ncku.edu.tw (C.-Y.K.); p68031018@mail.ncku.edu.tw (H.-C.K.)
[2]  Research Center for Environmental Changes, Academia Sinica, Taipei 11529, Taiwan; plihkimo@gmail.com
[3]  Division of Geodetic Science, School of Earth Sciences, Ohio State University, Columbus, OH 43210, USA;
    ckshum@osu.edu
[4]  State Key Laboratory of Geodesy and Earth's Dynamics, Institute of Geodesy and Geophysics, Chinese
    Academy of Sciences, Wuhan 430077, China
[5]  Center for Space and Remote Sensing Research, National Central University, Taoyuan 32001, Taiwan;
    khtseng@csrsr.ncu.edu.tw
[6]  Department of Soil and Water Conservation, National Chung Hsing University, Taichung 402, Taiwan;
    wca03056@ms2.wra.gov.tw
\*  Correspondence: p68001021@mail.ncku.edu.tw; Tel.: +886-06-275-7575 (ext. 63833-818)

**Abstract:** The Taiwanese government has established a complete tide gauge network along the coastline for accurate sea-level monitoring. In this study, we analyze several factors impacting the determination of absolute or geocentric sea-level trends—including ocean tides, inverted barometer effect, datum shift, and vertical land motion—using tide gauge records near Taiwan, from 1993–2015. The results show that datum shifts and vertical land motion have a significant impact on sea-level trends with a respective average contribution of 7.3 and 8.0 mm/yr, whereas ocean tides and inverted barometer effects have a relatively minor impact, representing 9% and 14% of the observed trend, respectively. These results indicate that datum shifts and vertical land motion effects have to be removed in the tide gauge records for accurate sea-level estimates. Meanwhile, the estimated land motions show that the southwestern plain has larger subsidence rates, for example, the Boziliao, Dongshi, and Wengang tide gauge stations exhibit a rate of 24–31 mm/yr as a result of groundwater pumping. We find that the absolute sea-level trends around Taiwan derived from tide gauges or satellite altimetry agree well with each other, and are estimated to be 2.2 mm/yr for 1993–2015, which is significantly slower than the global average sea-level rise trend of 3.2 mm/yr from satellite altimeters. Finally, a recent hiatus in sea-level rise in this region exhibits good agreement with the interannual and decadal variabilities associated with the El Niño-Southern Oscillation and Pacific Decadal Oscillation.

**Keywords:** sea-level rise; satellite altimetry; tide gauge; vertical land motion

## 1. Introduction

The rise in global sea-levels resulting from global warming affects coastal ocean dynamics significantly, especially in heavily populated deltaic regions and islands [1]. Many studies of absolute global sea-level rise have indicated that the global rise rate was 1.0–2.4 mm/yr in the twentieth century [2–5]. Besides, from 1993 to 2009 the rates of global mean sea-level rise directly derived from tide gauges and satellite altimeters were $2.8 \pm 0.8$ and $3.2 \pm 0.4$ mm/yr, respectively [5]. However,
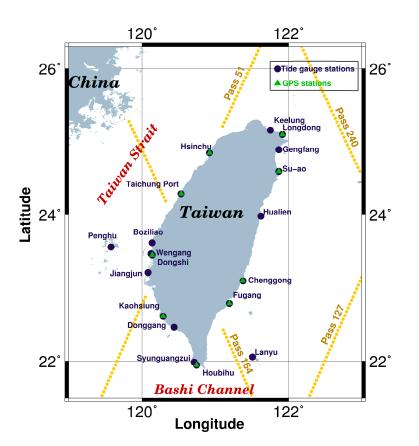
regional sea-level variations that deviate from the global average rate remain poorly understood [6]. Taiwan is a small island situated in the western Pacific, which is prone to floods, storm surges, and coastal hazards. Its topography is mainly formed with alluvial plains and central high mountains. Most densely populated cities are located 10–30 km from the shore. Thus, the present and future sea-level rise poses relatively serious effects for Taiwan as compared with other continental regions [7]. However, the rate of absolute sea-level change around Taiwan remains largely poorly determined. Some studies have suggested that the rate is significantly faster than the global average [8–11].

To estimate coastal sea-level trends over a multi-decadal time scale, tide gauges are the traditional means. However, only a few studies have focused on monitoring sea-level rise rates around Taiwan using tide gauges, and the estimated trends are significantly inconsistent with the results from satellite altimetry [7,8]. The primary reasons for this include the poor knowledge of crustal land motion and datum shifts in tide gauge records. Chen et al. [12] and Ching et al. [13] used a precise leveling survey and the Global Positioning System (GPS), respectively, to analyze land movement in Taiwan. Their results revealed significant vertical land motions which are much larger than neighboring sea-level trends on the southwestern and northeastern coast of Taiwan. Huang et al. [7] estimated sea-level trends by using a linear regression analysis to fit five tide gauge records (Keelung, Taichung, Jiangjun, Syunguangzui, and Fugang stations, illustrated in Figure 1) along the coast, and TOPEX/Poseidon and Jason-1/2 altimetric data close to these five tide gauges. Huang et al. [7] indicated that the trends derived from satellite altimetry were 3.1–6.6 mm/yr from 1992 to 2009, while the rates from the tide gauge records in the same period were 4.3–55.6 mm/yr. The maximum trend, at 55.6 mm/yr, was calculated using the Fugang tide gauge data (Figure 1). Huang et al. [7] suggested that uncorrected vertical land motion in tide gauge records resulted in the large discrepancy. Tseng et al. [8] analyzed sea-level variations in the same location by using tide gauges and the TOPEX/Poseidon satellite altimeter, and the results showed that the trend near the Taiwan Strait and Bashi Channel was 5.3 mm/yr as derived from altimetric data, while tide gauge records indicated a trend of 0–17 mm/yr from 1993 to 2003. The maximum trend of 17 mm/yr was calculated using the Penghu tide gauge data (Figure 1). The dataset was apparently polluted by significant vertical land motion. In addition, multiple jumps were observed in the records as a result of several undetected and uncorrected datum shifts (see Figure 3 of Tseng et al. [8]).

Hence, only a few studies have attempted to estimate the sea-level trend using tide gauges along the Taiwanese coast, and the published results do not reflect the absolute sea-level trend, which contains land motion due to geophysical or human factors. The absolute sea-level trends defined in this study are the combined trends from steric sea-level and ocean mass components, which can be obtained from satellite altimetry [14–16]. For the determination of absolute sea-level trends from tide gauge records, in addition to the factors of datum and vertical motion mentioned above, the effects of ocean tides and atmospheric pressure also need to be removed from the tide gauge records to avoid uncertain sea-level trend calculations [17,18] and to be consistent with the altimetry observations.

The Taiwanese government established a dense tide gauge network composed of ~19 stations along the coastline for monitoring sea surface heights, as depicted in Figure 1. However, tide gauge records have to be carefully and professionally checked before serving as a source for sea-level trend determination. In order to capture regional variability, we evaluate sea-level change over a time span from 1993 to 2015 by utilizing all available tide gauges along the coastline instead of selecting only some specific stations as provided by Huang et al. [7] and Tseng et al. [8]. In addition, impacts from vertical land motion, datum shift, ocean tides, and inverted barometer effects on sea-level trends are analyzed. Finally, we present absolute sea-level trends around Taiwan using tide gauge and satellite altimeter data to evaluate the short-term changes associated with El Niño-Southern Oscillation (ENSO) and Pacific Decadal Oscillation (PDO).

**Figure 1.** Location of tide gauges (blue circle), global positioning system (GPS) stations (green triangle), and TOPEX/Poseidon ground tracks (yellow dotted line) used in this study.

## 2. Data Sets

### 2.1. Tide Gauge Records

The tide gauges used in this study are provided by three data agencies in Taiwan, namely, the Central Weather Bureau, the Water Resources Agency, and the Harbor and Marine Technology Center. Figure 1 and Table 1 display these 18 stations along the coast of Taiwan and one station at the Penghu offshore islet. The gauges have unsynchronized sampling intervals of 6 min, 10 min, or hourly. Although the start dates of the records used in this study vary, most of these tide gauges remained operational in 2015 (Table 1). To avoid the reduced accuracy of sea-level estimates, all gauges had at least 15 years of data [19,20]. Moreover, pre-processing of the raw observations was required to ensure that the data was free of external influences. The quality control included visual and statistical checks of the tide gauge time series. The daily values were calculated with a simple average of all available raw values in a day if <30% records in that day were missing. Likewise, the monthly values were calculated from the daily data with a simple average of all the available daily values in a month if <30% values in that month were missing (following the rule of quality control from the University of Hawaii Sea Level Center (UHSLC)). In addition, tide gauge stations were excluded if their valid records were less than 70% in a >15-year time span or included nonlinear vertical motion as compared with neighboring tide gauges and altimetric measurements.

**Table 1.** Absolute sea-level trends and vertical motion rates obtained in this study.

| Station Name | Data Period | Coordinates | | Absolute Sea-Level Trend (mm/yr) | | Vertical Land Motion Rates (mm/yr) | | GPS Period | Dist. (*km*) | *C.C.* |
|---|---|---|---|---|---|---|---|---|---|---|
| | | Lat. (° N) | Lon. (° E) | Tide gauge (TG) | Altimetry 1993–2015 | ALT–TG | GPS | | | |
| Keelung (KL) | 1993–2015 | 25.155 | 121.752 | 2.7 ± 0.3 (±0.6) | 2.3 ± 0.3 | 1.5 ± 0.5 | N/A | N/A | N/A | 0.73 |
| Longdong (LD) | 2001–2015 | 25.098 | 121.918 | 1.6 ± 0.6 (±1.1) | 2.4 ± 0.3 | −2.5 ± 0.9 | −3.5 ± 0.1 | 2003–2012 | 0.01 | 0.73 |
| Gengfang (GF) | 1993–2008 | 24.892 | 121.869 | 3.5 ± 0.6 (±0.9) | 2.4 ± 0.3 | 4.2 ± 0.7 | N/A | N/A | N/A | 0.62 |
| Su-ao (SA) | 1997–2015 | 24.593 | 121.867 | 1.1 ± 0.4 (±0.6) | 2.3 ± 0.3 | −5.2 ± 0.5 | −4.6 ± 0.1 | 2002–2012 | 0.02 | 0.68 |
| Hualien (HL) | 1997–2015 | 23.981 | 121.624 | −0.5 ± 0.5 (±1.1) | 1.9 ± 0.5 | −6.2 ± 1.0 | N/A | N/A | N/A | 0.25 |
| Chenggong (CHG) | 1993–2015 | 23.097 | 121.380 | 1.3 ± 0.4 (±1.0) | 2.0 ± 0.6 | −2.1 ± 0.9 | 1.5 ± 0.1 | 2002–2012 | 0.60 | 0.20 |
| Fugang (FG) | 1993–2015 | 22.791 | 121.192 | 2.9 ± 0.4 (±0.6) | 2.2 ± 0.5 | 1.8 ± 0.5 | −1.2 ± 0.1 | 2003–2012 | 0.00 | 0.57 |
| Lanyu (LY) | 2001–2015 | 22.058 | 121.507 | 1.9 ± 1.1 (±1.3) | 3.0 ± 0.5 | −0.4 ± 0.7 | N/A | N/A | N/A | 0.85 |
| Houbihu (HBH) | 1998–2015 | 21.946 | 120.745 | 1.6 ± 0.8 (±1.5) | 2.5 ± 0.5 | −17.8 ± 1.3 | −23.4 ± 0.3 | 2009–2012 | 0.32 | 0.23 |
| Syunguangzui (SGZ) | 1993–2015 | 21.986 | 120.712 | 2.4 ± 0.4 (±0.7) | 2.5 ± 0.5 | −10.3 ± 0.6 | N/A | N/A | N/A | 0.49 |
| Donggang (DG) | 1998–2015 | 22.465 | 120.438 | 2.8 ± 0.7 (±1.0) | 2.2 ± 0.4 | −5.7 ± 0.7 | N/A | N/A | N/A | 0.73 |
| Kaohsiung (KS) | 1993–2014 | 22.614 | 120.288 | 2.7 ± 0.4 (±0.6) | 2.2 ± 0.4 | 0.6 ± 0.4 | −0.9 ± 0.1 | 2004–2012 | 0.01 | 0.82 |
| Jiangjun (JG) | 1993–2015 | 23.213 | 120.083 | 2.5 ± 0.5 (±0.7) | 2.2 ± 0.4 | −3.1 ± 0.5 | N/A | N/A | N/A | 0.69 |
| Dongshi (DS) | 1993–2015 | 23.450 | 120.139 | 2.4 ± 0.5 (±0.9) | 2.3 ± 0.5 | −31.0 ± 0.7 | −32.4 ± 0.1 | 2004–2012 | 0.27 | 0.43 |
| Wengang (WG) | 1993–2015 | 23.467 | 120.123 | 1.8 ± 0.6 (±1.1) | 2.4 ± 0.5 | −23.5 ± 0.9 | N/A | N/A | N/A | 0.43 |
| Penghu (PH) | 1993–2015 | 23.560 | 119.577 | 2.2 ± 0.4 (±0.6) | 2.4 ± 0.4 | 5.6 ± 0.4 | N/A | N/A | N/A | 0.70 |
| Boziliao (BZL) | 1995–2015 | 23.619 | 120.138 | 2.1 ± 0.6 (±1.1) | 2.5 ± 0.5 | −26.8 ± 0.9 | N/A | N/A | N/A | 0.37 |
| Taichung Port (TCP) | 1993–2015 | 24.288 | 120.533 | 3.7 ± 0.5 (±1.2) | 3.2 ± 0.8 | −3.9 ± 1.1 | −3.3 ± 0.1 | 2004–2012 | 0.39 | 0.44 |
| Hsinchu (HSC) | 1993–2015 | 24.849 | 120.921 | 2.8 ± 0.4 (±1.2) | 2.9 ± 0.8 | 1.0 ± 1.1 | −3.3 ± 0.1 | 2004–2012 | 0.42 | 0.23 |
| Mean | 1993–2015 | | | 2.2 | 2.2 ± 0.3 | −6.5 | −7.9 | 2002–2012 | 0.23 | 0.54 |

Note: Lat. and lon. represent latitude and longitude, respectively. N/A represents no GPS station close to the tide gauge sites. The positive value in vertical land motion represents uplift, and negative means subsidence. *C.C.* refers to correlation coefficient. Column 5 regarding TG estimates shows two kinds of standard deviations; one is calculated by least squares adjustment, and the other in brackets is calculated using the standard deviations of the relative sea-level trends and vertical land motion rates by error propagation theory.

### 2.2. Satellite Altimetric Data

Satellite altimetry has provided high-quality and global observations of sea surface heights since the early 1990s. It has been widely agreed that satellite altimetry provides a synoptic view of global ocean circulation and mesoscale variabilities. The along-track, time-delayed sea-level anomaly data used in this study were obtained from the Archiving, Validation, and Interpretation of Satellite Oceanographic (AVISO) data center, including TOPEX/Poseidon and Jason-1/2 (http://www.aviso.altimetry.fr/en/home.html). The AVISO data were processed with instrument, medium (ionospheric, wet, and dry tropospheric), and geophysical corrections (solid earth, polar, ocean and load tides, sea state bias, and inverted barometer correction). In order to combine it with tide gauge data to determine the vertical crustal motion at the tide gauges and the sea-level rise, the along-track altimetric data within 2° of each tide gauge location was utilized to generate monthly average time series using the weight from the square of the reciprocal of the distance. Given that sea-level trends are non-uniform around Taiwan [7], the along-track altimetric data were divided into the east coast (Pacific Ocean) and the west coast (Taiwan Strait) of Taiwan along the line of longitude 121° E, and we used altimetric data from the east or west part of Taiwan to compute the sea-level variations in combination with the tide gauges located along the east or west coasts.

### 2.3. Climate Indices

To investigate the rate of sea-level change around Taiwan and how it is affected by low-frequency climate variability, two climate indices were used in this study. The Southern Oscillation Index (SOI) was selected to represent ENSO variability [21,22], which is based on the observed sea-level pressure differences between Tahiti and Darwin, Australia. Prolonged periods of negative SOI values indicate El Niño episodes, and positive values are associated with La Niña events. The other index is PDO, which is highly correlated with ENSO episodes but for a longer period. The PDO index is defined as the leading principal component of monthly sea surface temperature anomalies in the North Pacific basin (poleward of 20° N in 1900–1993), and the PDO index covering the period from 1948 to 2015 can be downloaded from the Joint Institute for the Study of the Atmosphere and Ocean, University of Washington (http://research.jisao.washington.edu/pdo/PDO.latest) [23,24]. We applied an eleven-month and five-year moving average for the SOI and PDO indices, respectively, to clearly describe the interannual characteristics of these two indicators.

## 3. Tide Gauge Processing

Tide gauge data is prone to being contaminated by anomalous jumps owing to external forces and environmental changes, aside from natural variabilities. Hence, we calculated and analyzed the contributions of a variety of factors of sea-level trends, including ocean tides, static atmospheric pressure loading (or inverted barometer (IB) effect), datum shifts, and vertical land motions at the tide gauge sites. We applied corrections to the tide gauge data sequentially as follows: ocean tides, IB effect, datum shifts, and vertical land motions. This approach was selected because the tide gauge data used in this study include high-frequency signals and require correction for datum and vertical land motion combined with satellite altimeter data.

### 3.1. Ocean Tides

Ocean tides, or astronomical tides, are caused by the changing positions of celestial bodies and result in the tidal periodicity phenomenon. Theoretically, ocean tides are composed of an infinite number of tidal constituents, but the main tidal constituents are usually applied to analyze local ocean tides. A number of studies have utilized the moving average method or harmonic analysis [25] to correct the tide gauge records for ocean tides. In this study, to avoid the influence of datum shift errors on the section of tide gauge records through the moving average method, harmonic analysis was

applied to correct the effect of ocean tides in the tide gauge records. The original tide gauge records, *TG*, can be expressed as

$$TG(t) = a_0 + \sum_{i=1}^{m} a_i H(t - t_{a_i}) + bt + \sum_{j=1}^{n} \left[ A_j \sin(\omega_j t) + B_j \cos(\omega_j t) \right], \tag{1}$$

$$H(t - t_{a_i}) = \begin{cases} 1 & , & t \geq t_{a_i} \\ 0 & , & t < t_{a_i} \end{cases}$$

where $a_0$ and $b$ are the bias and the rate of relative sea-level change, respectively. $a_j$ is the $i$th datum shift in the tide gauge records, and $H$ is a step function. The amplitudes, $C_i$, for a particular tidal constituent frequency, $\omega_j$, can be derived from the combination of sine and cosine amplitudes, $A_j$ and $B_j$ ($C_i = (A_j^2 + B_j^2)^{1/2}$). $\omega_j$ represent the major tidal constituent frequency ($n = 37$), including eighth-diurnal constituents (M8), sixth-diurnal constituents (M6 and S6), quarter-diurnal constituents (MN4, S4, M4, and MS4), third-diurnal constituents (M3, MK3, and 2MK3), semi-diurnal tides (M2, S2, N2, K2, L2, T2, R2, MU2, NU2, 2N2, LAM2, and 2SM2), diurnal tides (K1, O1, P1, Q1, OO1, S1, M1, J1, RHO1, and 2Q1), the long-term tides (Mm, MSf, and Mf), and the annual term Sa and semi-annual term Ssa [26]. In this study, the unknown coefficients in Equation (1) were estimated by the least squares method. Then, we removed the fitted ocean tides, excluding the annual and semi-annual signals, from the tide gauge records.

### 3.2. Atmospheric Pressure Loading

The effect of atmospheric pressure loading is evident in the global ocean, except for in the tropics and the western boundary current extension regions [27]. Therefore, we aimed to correct the IB effect on tide gauge records in this study. The *IB* effect can be expressed as

$$IB = -9.948 \times (P_{atm} - P) \tag{2}$$

where *9.948* is a scale factor derived from the theoretical value at mid-latitudes [28,29], $P_{atm}$ is the sea surface pressure, and *P* is the monthly average sea-level pressure obtained over the global ocean. To correct the IB effect on tide gauge records, we used the global monthly mean sea-surface pressure field during the period from 1979–2015 with a spatial resolution of $0.75° \times 0.75°$ from the European Centre for Medium-Range Weather Forecasts (ECMWF) [30] (downloaded from http://www.ecmwf.int/). Considering the discrepancy of temporal sampling—6 min, 10 min, or hourly for the tide gauge data and six-hourly for the sea-level pressure field—from the ECMWF, the daily means of the sea-level changes and the sea surface pressures were computed from the tide gauges and the ECMWF data, respectively, to correct the IB effect on tide gauge records. Several studies indicate that IB effect has to be corrected in tide gauge records [27,29,31], and it mainly influences seasonal sea-level variations (annual and semi-annual cycles) [31,32]. Therefore, daily data is dense enough to capture IB influences. In addition, the ECMWF sea-surface pressure data used in this study have been compared with the in-situ observed pressure data from the Central Weather Bureau of Taiwan, and both agree well (not shown here).

### 3.3. Datum Shifts in the Tide Gauge Records

The tide gauge stations measure sea-level heights accurately relative to a nearby geodetic benchmark (local datum), but the tide gauge records could contain uncorrected datum shifts that will affect sea-level trend determination because of natural disasters, human errors, or poor maintenance. However, the agency responsible for managing tide gauge stations does not provide the supporting documentation showing the maintenance dates for instrument repair or replacement. Therefore, all tide gauge records have to be carefully checked for possible datum shifts.

The data used for datum shift detection are the differences between two records in two consecutive time periods (from one month to the previous in each of the tide gauge time series) [33]. However, multiple jumps could appear in the differences because of strong seasonal variations (annual and semi-annual) in the sea-level induced by monsoons and thermal expansion or sporadic storm surges (e.g., typhoons). Therefore, a two-step process was applied to the tide gauge records. The first step was to remove the seasonal signals in the monthly tide gauge time series through a six-parameter regression analysis (bias, trend, annual, and semi-annual terms) as depicted in Figure 2a (purple curve). The second step was to analyze the non-seasonal variations of the tide gauge data through the multiresolution analysis method [34,35]. Multiresolution analysis based on wavelet theory aims to remove high-frequency signals from the monthly tide gauge data. The multiresolution analysis method includes two important parameters, namely, wavelet functions, $\psi$, and scaling functions, $\phi$ which are used to find the signal details and approximations, respectively. We represent the tide gauge records, $f$, as an orthogonal series with $\psi$ and $\phi$

$$f(t) = \sum_k c_{j0}(k) 2^{j_0/2} \phi(2^{j_0}t - k) + \sum_k \sum_{j=j_0}^{\infty} d_j(k) 2^{j/2} \psi(2^j t - k) \tag{3}$$

where $t$ is the time, and $c$ and $d$ are the coefficients of low- and high-pass filters, respectively, which are computed using the discrete wavelet transformation [34,35]. $j$ and $k$ are the dilation and translation parameters. $j = j_0, j_0 + 1, \dots, J - 1$ and $j_0$ and $J$ are the coarsest and finest levels, respectively.

Multiresolution analysis is used to numerically decompose and reconstruct a signal. We applied the Haar wavelet to decompose the tide gauge data down to the third ($j = J - 3$) or fourth ($j = J - 4$) level depending on the length of the tide gauge data and then to reconstruct the denoised, nonseasonal tide gauge data (red curve in Figure 2b).

The reconstructed low-pass data were then used to calculate the differences between the two adjacent times (one month to the previous in each of the time series). A difference larger than 50 mm was automatically considered a suspected datum shift (green stars in Figure 2c). To discover the actual datum shifts from the suspected datum shifts derived from the previous step, we averaged the two-year records before and after the epoch of the suspected shift using the deseasonal data (purple curve in Figure 2a) and calculated the difference of these two means. If the difference was significantly larger than 100 mm (the threshold), then the jump was considered a datum shift (star in Figure 2d). If the difference approximated 100 mm, then the data were compared with the neighboring tide gauges and altimetric data for a double check. To get the two threshold values mentioned above, we analyzed sea-level variations around Taiwan derived from the along-track altimetric data by using the same procedure of datum shift detection applied to the tide gauges.

The vertical land motion at the tide gauge stations was determined by a classic approach using the differences of altimetric and tide gauge data [19,36,37], which is expressed as:

$$u(\lambda, \varphi, t) = alt(\lambda, \varphi, t) - TG(\lambda, \varphi, t) \tag{4}$$

where $u$ is the vertical land motion; $alt$ is the altimetric data; $TG$ is the tide gauge records; $\lambda$ and $\phi$ are the latitude and longitude, respectively; and $t$ is time.
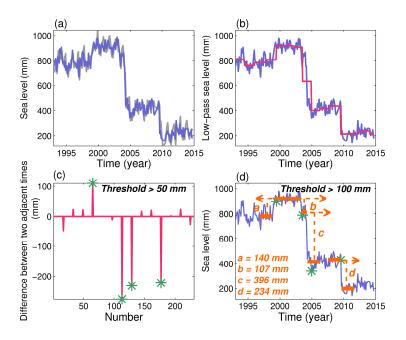
The vertical motion and datum shifts are then estimated by fitting a linear regression as follows:

$$u(t) = a_0 + \sum_{i=1}^{m} a_i H(t - t_{a_i}) + b\prime t \tag{5}$$

$$H(t - t_{a_i}) = \begin{cases} 1 & , \quad t \geq t_{a_i} \\ 0 & , \quad t < t_{a_i} \end{cases}$$

where $a_o$ and $b\prime$ are the bias and the rate of vertical motion, respectively; $a_i$ is the $i$th datum shift ($m$: the number of datum shifts); and $H$ is the step function.



**Figure 2.** Detection of datum shifts in the monthly Kaohsiung tide gauge records. (**a**) original and deseasonal sea-level changes (original: gray line; deseasonal: purple line); (**b**) low-pass sea-levels based on the Haar multiresolution analysis (red line); (**c**) the differences between the two values in the adjacent times using the red line data in (**b**) (one month to the previous in each of the time series), the green stars are the suspected datum shifts (>50 mm); (**d**) the difference between the two averages that are calculated using the two-year records before and after the suspected datum shift.

## 3.4. Vertical Land Motion Derived from Altimetry and Tide Gauge Data

On the southwestern coast of Taiwan, vertical ground motions could be significantly larger than neighboring sea-level variations because of a number of geophysical processes and human activities, such as groundwater pumping [12,13]. Vertical land motions have to be corrected in tide gauge records to obtain the absolute sea-level changes. In previous studies, e.g., [12,38], glacial isostatic adjustment (GIA) models, leveling, and GPS observations were used for vertical motion correction. However, leveling and GPS measurements are unavailable at all tide gauges in Taiwan, and the magnitude of the GIA effect around Taiwan is about 0.1 mm/yr and is negligible [39], because the effect is much smaller than the realistic motions due to other geophysical processes [40]. Tide gauge records contain vertical land motions and absolute sea-levels, whereas satellite altimeters observe geocentric sea-level changes only. Therefore, the vertical land motions at the tide gauge stations can be estimated by the classic approach as expressed previously in Equations (4) and (5) using a combination of the altimetric and tide gauge data [19,36]. Then, we used the estimated land motion rates to correct tide gauge records to determine the absolute sea-level rise.

A total of 199 continuous GPS observations covering 2002–2012 were used to validate our estimates of vertical land motion (updated from Ching et al. [13]). The GPS stations were selected as closely as possible to the tide gauge sites, and the threshold of the distance between the tide gauge and the continuous GPS station was set at 1 km (Table 1).

## 4. Results and Discussion

### 4.1. Impacts of Geophysical and Datum Shift Corrections on Sea-Level Trends

Our processed Keelung and Kaohsiung tide gauge records were compared with those from the UHSLC data to evaluate our data processing. The Kaohsiung tide gauge records agree well, but the Keelung data show a discrepancy from 1999–2001 and 2003–2005 because of large data gaps. The sea-level trends determined using tide gauges with different geophysical and datum corrections in 1993–2015 are displayed in Table 2. The sea-level trends derived from the original data with or without ocean tides and IB corrections have no significant trend differences, which are in the ranges of −0.9–0.8 and −0.6–0.4 mm/yr, respectively, and are nearly smaller than or equal to the average standard deviation of the trend of 0.8 mm/yr. The average trends changed from 5.9 to 8.7 mm/yr when the datum shift was applied to the tide gauge data and from 8.7 to 2.2 mm/yr when the land motion was corrected. The standard deviation of the trends reduced to approximately 0.5 mm/yr. This result implies the significant contributions of datum shift and vertical land motion corrections to sea-level change around Taiwan. The relative sea-level trends corrected for datum shifts are geographically nonuniform. Higher rates of relative sea-level trends (>20 mm/yr) appear in southwest Taiwan (Table 2), which may be associated with land subsidence (discussed later). After all the corrections were applied (including ocean tides, IB, datum, and vertical land motions), the absolute sea-level trends around Taiwan using the tide gauge data covering 1993–2015 show a range from −0.5 to 3.7 mm/yr (Table 2).
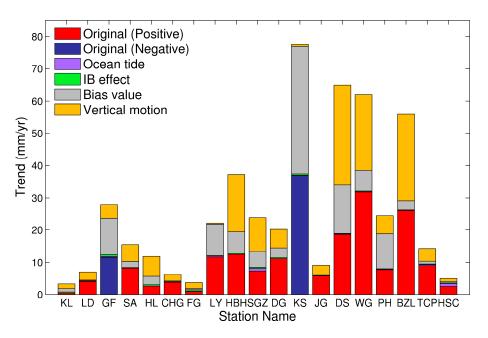
**Table 2.** Sea-level trends derived from tide gauges with different geophysical and datum corrections applied.

| Station Name | Trend (mm/yr) | | | | |
| --- | --- | --- | --- | --- | --- |
| | Original | With Ocean Tides Correction | With Ocean Tides and IB Corrections | With Ocean Tides, IB, and Datum Corrections | With Ocean Tides, IB, Datum, and Vertical Land Motion Corrections ** |
| Keelung (KL) | 0.5 ±0.5 | 0.5 ± 0.5 | 0.2 ± 0.5 | 1.2 ± 0.3 | 2.7 ± 0.3 (±0.6) |
| Longdong (LD) | 4.1 ± 0.7 | 4.3 ± 0.7 | 4.1 ± 0.6 | 4.1 ± 0.6 * | 1.6 ± 0.6 (±1.1) |
| Gengfang (GF) | −11.6 ± 1.0 | −11.4 ± 0.9 | −12.0 ± 0.9 | −0.8 ± 0.6 | 3.5 ± 0.6 (±0.9) |
| Su-ao (SA) | 8.2 ± 0.7 | 8.3 ± 0.6 | 8.2 ± 0.6 | 6.3 ± 0.4 | 1.1 ± 0.4 (±0.6) |
| Hualien (HL) | 2.6 ± 0.7 | 2.6 ± 0.7 | 3.0 ± 0.7 | 5.7 ± 0.5 | −0.5 ± 0.5 (±1.1) |
| Chenggong (CHG) | 3.8 ± 0.5 | 3.6 ± 0.5 | 3.4 ± 0.4 | 3.4 ± 0.4 * | 1.3 ± 0.4 (±1.0) |
| Fugang (FG) | 1.0 ± 0.5 | 1.1 ± 0.5 | 0.7 ± 0.5 | 1.1 ± 0.4 | 2.9 ± 0.4 (±0.6) |
| Lanyu (LY) | 11.7 ± 1.3 | 12.0 ± 1.3 | 11.9 ± 1.2 | 2.2 ± 1.1 | 1.9 ± 1.1 (±1.3) |
| Houbihu (HBH) | 12.5 ± 1.3 | 12.5 ± 1.2 | 12.8 ± 1.2 | 19.4 ± 0.8 | 1.6 ± 0.8 (±1.5) |
| Syunguangzui (SGZ) | 7.3 ± 0.6 | 8.1 ± 0.6 | 7.7 ± 0.6 | 12.7 ± 0.4 | 2.4 ± 0.4 (±0.7) |
| Donggang (DG) | 11.2 ± 0.8 | 11.2 ± 0.8 | 11.5 ± 0.7 | 8.5 ± 0.7 | 2.8 ± 0.7 (±1.0) |
| Kaohsiung (KS) | −36.9 ± 1.7 | −37.0 ± 1.7 | −37.4 ± 1.6 | 2.1 ± 0.4 | 2.7 ± 0.4 (±0.6) |
| Jiangjun (JG) | 5.8 ± 0.5 | 5.8 ± 0.5 | 5.6 ± 0.5 | 5.6 ± 0.5 * | 2.5 ± 0.5 (±0.7) |
| Dongshi (DS) | 18.6 ± 0.9 | 18.4 ± 0.9 | 18.3 ± 0.9 | 33.4 ± 0.5 | 2.4 ± 0.5 (±0.9) |
| Wengang (WG) | 31.8 ± 1.1 | 31.9 ± 1.1 | 31.7 ± 1.1 | 25.3 ± 0.6 | 1.8 ± 0.6 (±1.1) |
| Penghu (PH) | 7.7 ± 0.6 | 7.5 ± 0.6 | 7.4 ± 0.6 | −3.4 ± 0.4 | 2.2 ± 0.4 (±0.6) |
| Boziliao (BZL) | 26.0 ± 1.1 | 26.1 ± 1.0 | 26.0 ± 1.0 | 28.9 ± 0.6 | 2.1 ± 0.6 (±1.1) |
| Taichung Port (TCP) | 9.0 ± 0.7 | 8.7 ± 0.6 | 8.5 ± 0.6 | 7.6 ± 0.5 | 3.7 ± 0.5 (±1.2) |
| Hsinchu (HSC) | 2.5 ± 0.7 | 1.6 ± 0.6 | 1.4 ± 0.6 | 1.8 ± 0.4 | 2.8 ± 0.4 (±1.2) |
| Mean | 6.1 | 6.1 | 5.9 | 8.7 | 2.2 |

Note: * represents no datum shift detected in the tide gauge data. ** Columns 6 shows two standard deviations. One is calculated by least squares adjustment, and the other in brackets is calculated using the standard deviations of the relative sea-level trends and vertical land motion rates by the error propagation theory.

To illustrate the contributions of each geophysical and datum correction to sea-level variations around Taiwan, the absolute value of trend differences after the different corrections was calculated and is presented in Figure 3. The ocean tides change the sea-level trends in the range of 0–0.9 mm/yr, with a mean of 0.2 mm/yr, and the effect of the IB change ranges from 0.1 to 0.6 mm/yr, with a mean
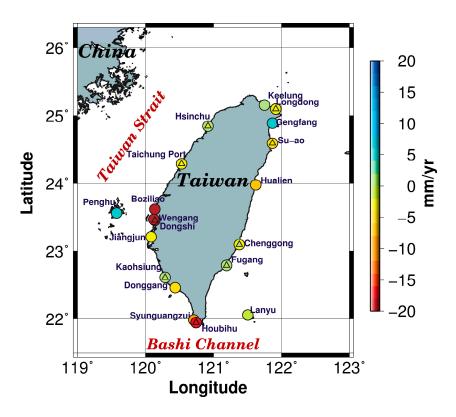
of 0.3 mm/yr. The results indicate that ocean tides and IB have a slight impact on sea-level trends around Taiwan, as determined by the tide gauges, constituting approximately 9% and 14% of the observed trend, respectively. The datum shift has a significant impact on sea-level trends as derived from the tide gauges at 0.4–39.5 mm/yr, with an average trend of 7.3 mm/yr; the vertical land motions contribute to the regional sea-level trends in the study area with a range of 0.4–31.0 mm/yr, with an average trend of 8.0 mm/yr (Figure 3). These values are significantly larger than the global mean sea-level rise of 3.2 ± 0.1 mm/yr [1] derived from satellite altimetry for 1993–2012, thereby indicating that they have to be considered when calculating absolute sea-level trends around Taiwan from tide gauge data.



**Figure 3.** Effects of each geophysical and datum shift correction on the sea-level trends around Taiwan using tide gauges covering 1993–2015.

Vertical motion correction is crucial in the Taiwan region because vertical motions along the southwestern and northeastern coasts of Taiwan are larger than sea-level trends [13]. The results of the estimated vertical motions for each station are illustrated in Figure 4. The results are geographically nonuniform. In the eastern area of Taiwan, the estimated vertical land motion trends indicate a range of −6.2–4.2 mm/yr; the maximum subsidence trend of 6.2 mm/yr is from the Hualien tide gauge data, where subsidence was observed at 10 mm/yr relative to Hualien City, using the space-borne synthetic aperture radar interferometry method for 2004–2008 [41]. The discrepancy between our result and the result from a previous study [41] may be caused by the observations covering different time periods. Significant subsidence was observed at the tide gauges in the western area of Taiwan, especially in the southwestern area of the Boziliao, Dongshi, and Wengang tide gauge sites, with rates of 23.5–31.0 mm/yr (Figure 4; see Supplementary Material for details about the Dongshi tide gauge records). This strong subsidence was also confirmed by GPS observations around Taiwan [13]. The southwestern plains of Taiwan are highly developed agricultural and fishery areas. Thus, land surface elevation falls gradually because of groundwater pumping in the southwestern plains [13,42].
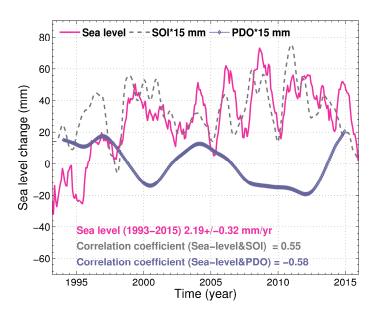
In Figure 4, the GPS and altimeter–tide gauge derived results agree well, and both results indicate land subsidence. The mean of the trend differences between the GPS and the altimeter-gauge derived vertical motion trends is 1.3 ± 2.8 mm/yr. The large standard deviations may be caused by the rare validation of GPS data. In Figure 4, the estimated vertical motion trend in Houbihu has a large discrepancy compared with the GPS velocity, which may be caused by the distance between the two stations at 0.23 km, and such an area could produce locally significant rates of vertical deformation [13].

**Figure 4.** Vertical land motion trends derived from combining data from altimetry and tide gauges (circle) and from GPS (triangle).

## 4.2. Mean Sea-Level Around Taiwan: Trend and Interannual Variability

The rates of absolute sea-levels around Taiwan from the tide gauge and satellite altimeter data for 1993–2015 are presented in Table 1. All tide gauge rates presented in this study agree well with the satellite altimeter. In 1993–2015, the average of the absolute sea-level trends around Taiwan derived from all coastal tide gauge data is 2.2 mm/yr, which is identical to the rate of $2.2 \pm 0.3$ mm/yr from the altimeter data covering the same time span within the latitude of 21–26° N and longitude of 119–123° E (Table 1). These regional rates are significantly lower than those estimated from the altimeter data (5.0 mm/yr from Tseng et al. [8]) for 1993–2007 and also slightly lower than the observed global mean of $3.2 \pm 0.1$ mm/yr during the period from 1993 to 2012 [1]. In Figure 5, it can be seen that the mean sea-level around Taiwan decreased significantly in 2014–2015. Thus, this discrepancy might have resulted from the different time periods for calculating the rates. In addition, comparing our estimates with the results of Feng and Tsimplis [10] indicates the trends derived from the tide gauges are 2.0–14.1 mm/yr with an average trend of 6.0 mm/yr from 1954 to 2012, the large discrepancy might have resulted from the uncorrected vertical land motion in tide gauge records and the data used covering different time spans.

**Figure 5.** Sea-level changes around Taiwan derived from the satellite altimetric data covering the time span from 1993 to 2015. The seasonal signals have been removed, and an 11-month smoothing applied to the altimetric data. The gray dashes and purple diamond curves denote the low-pass southern oscillation index (SOI) and Pacific decadal oscillation (PDO), respectively, using 11-month and five-year smoothing, respectively. The correlation coefficients were calculated by the Pearson method, and the *p*-value is <0.05.

Interannual sea-level variability is related to ENSO and PDO around Taiwan [43,44]. Figure 5 shows the interannual sea-level variability around Taiwan, derived from altimeter data that has been smoothed with an 11-month running mean, and overlaid with the low-pass filtered SOI and PDO (smoothed with the 11-month and five-year running mean, respectively). The sea-level anomalies around Taiwan present an increasing trend from 1993 to 2013, but an obvious decreasing trend after 2013, occurring when the PDO (SOI) index exhibits a negative (positive) trend. The comparison between the sea-level change and the SOI and PDO indexes implies that the interannual sea-level variability around Taiwan is highly correlated with the SOI and PDO (with a correlation coefficient of 0.55/−0.58). Both the SOI and PDO are associated with changes of sea-level pressure, trade winds, and ocean temperature. The IB effect has only a minor impact on sea-level trends around Taiwan, whereas the sea-level changes in the Western Pacific Ocean are mainly driven by trade wind and seawater density variations caused by ocean temperature and salinity changes, which increase when the SOI or PDO index manifests a positive or negative trend, respectively, and vice versa [45–47]. The absolute sea-level trend derived from the altimeter data covering 1993–2013 is 2.8 ± 0.4 mm/yr, while the rates decrease to 2.2 ± 0.3 mm/yr for 1993–2015. The difference between the regional rates of the sea-level rise during the two periods is 0.6 mm/yr, which is tested to be statistically significant at 90% confidence level. This result means that low-frequency variability strongly influences the regional sea-level around Taiwan, and the trend is mainly influenced by the PDO phenomenon, because the 10–30 study data span is longer than the data span of the altimeter [23]. The PDO shows a negative trend for 1993–2012, but a significantly positive trend after 2012 (Figure 5). Therefore, the PDO may undergo a phase shift as shown in Figure 5 [48], leading to lower sea-level trends around Taiwan in the next few decades. In addition, the 18.6-year nodal tide is not included in the harmonic analysis in this study, because it is not corrected in the AVISO altimetric data that was used and it would be small, especially in middle-latitude areas [49,50]. Cherniawsky et al. [49] indicated that the observed amplitudes of the 18.6-year nodal tide are about 1.5–3.5 cm, but theoretical amplitudes are less than 1 cm everywhere, suggesting that the difference results from part of the broad-band decadal ocean variability. In Taiwan, the amplitude of the 18.6-year nodal tidal cycle is about 3 mm [50]. We simulated

the influence of the 18.6-year nodal tide with an amplitude of 3 mm on trend analysis when the time series cover 15 years and 19 years. Results show trend changes of 0.5 mm/yr for a 15-year time series and 0.2 mm/yr for a 19-year time series, showing that this effect would be small when the records span a couple of decades [50]. In this study, 74% of the gauges we used cover a time span longer than 19 years.

## 5. Conclusions

In this study, we quantified the factors impacting the determination of absolute sea-level trends around coastal Taiwan using tide gauge records, including ocean tides, IB effect, datum shift, and vertical land motion. The ocean tides and IB effects had a marginal impact on the sea-level trends determined by the tide gauges, at 0–0.9 and 0.1–0.6 mm/yr, with average rates of 0.2 and 0.3 mm/yr, respectively. The datum shifts and vertical land motions had a significant impact on sea-level trends with an average of 7.3 and 8.0 mm/yr, respectively, thereby indicating that both effects require correction in the tide gauge records along the Taiwanese coast when estimating absolute sea-level trends using tide gauges. Therefore, GPS can be collocated when Taiwanese agencies establish new tide gauge stations for future absolute sea-level monitoring. The results of the estimated vertical motions show that land around Taiwan generally subsided during the period from 1993 to 2015 and that the southwestern area of Taiwan has a high subsidence rate, especially at the Boziliao, Dongshi, and Wengang tide gauge stations, with rates of 23.5–31.0 mm/yr. The increased groundwater pumping in the southwestern plains may exacerbate land subsidence [13,42], and in turn increase the rates of relative sea-level trend. In addition, we compared our estimates derived from the differences between the satellite altimeter and tide gauge data with the continuous GPS-measured rates for 2002–2012 [13], which agree well with the mean of the trend differences of $1.3 \pm 2.8$ mm/yr.

The sea-level trend around Taiwan covering the time span from 1993 to 2015 was 2.2 mm/yr as derived from the altimetric data; the tide gauge data also provided an estimated trend of 2.2 mm/yr in the same period. Both estimates agree well and are slower than the global average trend of 3.2 mm/yr [1], and the previous study estimates of 5.0 mm/yr from the altimeter data for 1993–2007 [8]. The recent slowing down of sea-level rise trends observed from 1993 to 2015 are found to be because trade winds are weak and a strong El Niño event occurred in 2015–2016, and the PDO underwent a phase shift (Figure 5). These results suggest that the regional sea-level trends around Taiwan in the next 10–30 years may be lower than the trends observed in the past 20 years. While the trends in the next few decades could be expected to be low, the long-term sea-level trends around Taiwan will continue to be affected by present and future global mean sea-level rise [48].

In summary, this study developed and demonstrated a robust procedure for the estimation of improved long-term regional sea-level trends, separating sea-level trend signal and land motion. We demonstrated that despite the unavailability of datum shift information to properly process long-term tide gauge data, our procedure proved to be robust via validation methods including statistical analysis and collocated GPS velocities. Although our procedure was demonstrated for and applied to coastal Taiwan, it could be used globally to improve regional sea-level trends.

of Taiwan, and the Harbor and Marine Technology Center of Taiwan. We also acknowledge the assistance of Kuo-En Ching with the GPS data processing.

## References

1. Cazenave, A.; Le Cozannet, G. Sea-level rise and its coastal impacts. *Earth's Future* **2014**, *2*, 15–34. [CrossRef]
2. Douglas, B.C. Sea-level change in the era of the recording tide gauge. In *Sea Level Rise—History and Consequences*; Douglas, B.C., Kearney, M.S., Leatherman, S.P., Eds.; Academic Press: San Diego, CA, USA, 2001; Volume 75, pp. 37–64.
3. Woodworth, P.L.; Teferle, F.N.; Bingley, R.M.; Shennan, I.; Williams, S.D.P. Trends in UK mean sea level revisited. *Geophys. J. Int.* **2009**, *176*, 19–30. [CrossRef]
4. Willis, J.; Chambers, D.P.; Kuo, C.Y.; Shum, C.K. Global Sea Level Rise: Recent Progress and Challenges for the Decade to Come. *Oceanography* **2010**, *23*, 26–35. [CrossRef]
5. Church, J.A.; White, N.J. Sea-level rise from the late 19th to the Early 21st Century. *Surv. Geophys.* **2011**, *32*, 585–602. [CrossRef]
6. White, N.J.; Haigh, I.D.; Church, J.A.; Koen, T.; Watson, C.S.; Pritchard, T.R.; Watson, P.J.; Burgette, R.J.; McInnes, K.L.; You, Z.J.; et al. Australian sea levels: Trends, regional variability and influencing factors. *Earth Sci. Rev.* **2014**, *136*, 155–174. [CrossRef]
7. Huang, C.J.; Hsu, T.W.; Wu, L.C. *Technology Development on Sea Level Change Estimation by In-Situ and Satellite Data (2/2)*; Water Resources Agency, R.O.C.: Taichung, Taiwan, 2010; pp. 1–302. (In Chinese)
8. Tseng, Y.H.; Breaker, C.L.; Chang, T.Y. Sea-level variations in the regional seas around Taiwan. *J. Oceanogr.* **2010**, *66*, 27–39. [CrossRef]
9. Liu, W.C.; Liu, H.M. Assessing the impacts of sea level rise on salinity intrusion and transport time scales in a tidal estuary, Taiwan. *Water* **2014**, *6*, 324–344. [CrossRef]
10. Feng, X.; Tsimplis, M.N. Sea level extremes at the coasts of China. *J. Geophys. Res. Oceans* **2014**, *119*, 1593–1608. [CrossRef]
11. Feng, X.; Tsimplis, M.N.; Woodworth, P.L. Nodal variations and long-term changes in the main tides on the coasts of China. *J. Geophys. Res. Oceans* **2015**, *120*, 1215–1232. [CrossRef]
12. Chen, K.H.; Yang, M.; Huang, Y.T.; Ching, K.E.; Rau, R.J. Vertical displacement rate field of Taiwan from geodetic levelling data 2000–2008. *Surv. Rev.* **2011**, *43*, 296–302. [CrossRef]
13. Ching, K.E.; Hsieh, M.L.; Johnson, K.M.; Chen, K.H.; Rau, R.J.; Ying, M. Modern vertical deformation rates and mountain building in Taiwan from precise leveling and continuous GPS observations, 2000–2008. *J. Geophys. Res.* **2011**, *116*. [CrossRef]
14. Willis, J.K.; Chambers, D.P.; Nerem, R.S. Assessing the globally averaged sea level budget on seasonal to interannual timescales. *J. Geophys. Res. Oceans* **2008**, *113*. [CrossRef]
15. Cazenave, A.; Dominh, K.; Guinehut, S.; Berthier, E.; Llovel, W.; Ramillien, G.; Ablain, M.; Larnicol, G. Sea level budget over 2003–2008: A reevaluation from GRACE space gravimetry, satellite altimetry and Argo. *Glob. Planet. Chang.* **2009**, *65*, 83–88. [CrossRef]
16. Leuliette, E.W.; Miller, L. Closing the sea level rise budget with altimetry, Argo, and GRACE. *Geophys. Res. Lett.* **2009**, *36*. [CrossRef]
17. Henry, O.; Prandi, P.; Llovel, W.; Cazenave, A.; Jevrejeva, S.; Stammer, D.; Meyssignac, B.; Koldunov, N. Tide gauge-based sea level variations since 1950 along the Norwegian and Russian coasts of the Arctic Ocean: Contribution of the steric and mass components. *J. Geophys. Res. Oceans* **2012**, *117*. [CrossRef]
18. Volkov, D.L.; Pujol, M.I. Quality assessment of a satellite altimetry data product in the Nordic, Barents, and Kara seas. *J. Geophys. Res. Oceans* **2012**, *117*. [CrossRef]
19. Kuo, C.Y.; Shum, C.K.; Braun, A.; Cheng, K.C.; Yi, Y. Vertical Motion determined using Satellite Altimetry and tide Gauges. *Terr. Atmos. Ocean. Sci.* **2008**, *19*, 21–35. [CrossRef]

20. Ray, R.D.; Beckley, B.D.; Lemoine, F.G. Vertical crustal motion derived from satellite altimetry and tide gauges, and comparisons with DORIS measurements. *Adv. Space Res.* **2010**, *45*, 1510–1522. [CrossRef]

21. Walker, G.T. Correlation in seasonal variations of weather, VIII: A preliminary study of world weather. *Mem. Indian Meteorol. Dep.* **1923**, *24*, 75–131.

22. Montgomery, R.B. Report on the work of G.T. Walker. *Mon. Weather Rev.* **1940**, *68*, 1–26.

23. Mantua, N.J.; Hare, S.R.; Zhang, Y.; Wallace, J.M.; Francis, R.C. A Pacific interdecadal climate oscillation with impacts on salmon production. *Bull. Am. Meteorol. Soc.* **1997**, *78*, 1069–1079. [CrossRef]

24. Zhang, Y.; Wallace, J.M.; Battisti, D.S. ENSO-like interdecadal variability: 1900–93. *J. Clim.* **1997**, *10*, 1004–1020. [CrossRef]

25. Parker, B. Tides. In *Encyclopedia of Coastal Science*; Schwartz, M.L., Ed.; Springer: Dordrecht, The Netherlands, 2005; pp. 987–996.

26. Chang, E.T.Y.; Chao, B.F.; Chiang, C.C.; Hwang, C. Vertical crustal motion of active plate convergence in Taiwan derived from tide gauge, altimetry, and GPS data. *Tectonophysics* **2012**, *578*, 98–106. [CrossRef]

27. Wunsch, C.; Stammer, D. Atmospheric loading and the oceanic "inverted barometer" effect. *Rev. Geophys.* **1997**, *35*, 79–107. [CrossRef]

28. Wunsch, C. Bermuda sea-level in relation to tides, weather and baroclinic fluctuations. *Geophys. Space Phys.* **1972**, *10*, 1–49. [CrossRef]

29. Dalrymple, R.A.; Breaker, L.C.; Brooks, B.A.; Cayan, D.R.; Griggs, G.B.; Han, W.; Horton, B.P.; Hulbe, C.L.; McWilliams, J.C.; Mote, P.W.; et al. *Sea-Level Rise for the Coasts of California, Oregon, and Washington: Past, Present, and Future*; The National Academies Press: Washington, DC, USA, 2012; pp. 1–217.

30. Dee, D.P.; Uppala, S.M.; Simmons, A.J.; Berrisford, P.; Poli, P.; Kobayashi, S.; Andrae, U.; Balmaseda, M.A.; Balsamo, G.; Bauer, P.; et al. The ERA-Interim reanalysis: Configuration and performance of the data assimilation system. *Q. J. R. Meteorol. Soc.* **2011**, *137*, 553–597. [CrossRef]

31. Ponte, R.M. Low-frequency sea level variability and the inverted barometer effect. *J. Atmos. Ocean. Technol.* **2006**, *23*, 619–629. [CrossRef]

32. Patullo, J.; Munk, W.; Revelle, R.; Strong, E. The seasonal oscillation in sea level. *J. Mar. Res.* **1955**, *14*, 88–155.

33. Church, J.A.; White, N.J.; Coleman, R.; Lambeck, K.; Mitrovica, J.X. Estimates of regional distribution of sea-level rise over the 1950-2000 period. *J. Clim.* **2004**, *17*, 2609–2625. [CrossRef]

34. Mallat, S.G. Multiresolution approximations and wavelet orthonormal bases of $L^2(R)$. *Trans. Am. Math. Soc.* **1989**, *315*, 69–89. [CrossRef]

35. Chicken, E.; Loper, D.E.; Werner, C.L. Estimating tidal effects in spring discharge: A multiscale method using correlated phenomena. *Water Resour. Res.* **2007**, *43*. [CrossRef]

36. Kuo, C.Y.; Shum, C.K.; Braun, A.; Mitrovica, J.X. Vertical crustal motion determined by satellite altimetry and tide gauge data in Fennoscandia. *Geophys. Res. Lett.* **2004**, *31*, 4–7. [CrossRef]

37. Wöppelmann, G.; Marcos, M. Coastal sea-level rise in southern Europe and the nonclimate contribution of vertical land motion. *J. Geophys. Res.* **2012**, *117*. [CrossRef]

38. Yildiz, H.; Andersen, O.B.; Simav, M.; Aktug, B.; Ozdemir, S. Estimates of vertical land motion along the southwestern coasts of Turkey from coastal altimetry and tide gauge data. *Adv. Space Res.* **2013**, *51*, 1572–1580. [CrossRef]

39. Wang, H.S.; Wu, P.; Jia, L.L.; Hu, B.; Jiang, L.M. The role of glacial isostatic adjustment in the present-day crustal motion and sea levels of East Asia. *Earth Planets Space* **2011**, *63*, 915–928. [CrossRef]

40. Woodworth, P.L. Some important issues to do with long-term sea level change. *Philos. Trans. R. Soc. A* **2006**, *364*, 787–803. [CrossRef] [PubMed]

41. Yen, J.Y.; Lu, C.H.; Chang, C.P.; Hooper, A.J.; Chang, Y.H.; Liang, W.T.; Chang, T.Y.; Lin, M.S.; Chen, K.S. Investigating active deformation in the northern Longitudinal Valley and City of Hualien in eastern Taiwan using persistent scatterer and small-baseline SAR interferometry. *Terr. Atmos. Ocean. Sci.* **2011**, *22*, 291–304. [CrossRef]

42. Kuo, C.Y.; Cheng, Y.J.; Lan, W.H.; Kao, H.C. Monitoring Vertical Land Motions in Southwestern Taiwan with Retracked Topex/Poseidon and Jason-2 Satellite Altimetry. *Remote Sens.* **2015**, *7*, 3808–3825. [CrossRef]

43. Zhang, X.; Church, J.A. Sea-level trends, interannual and decadal variability in the Pacific Ocean. *Geophys. Res. Lett.* **2012**, *39*. [CrossRef]

44. Cheng, Y.C.; Ezer, T.; Hamlington, B.D. Sea Level Acceleration in the China Seas. *Water* **2016**, *8*. [CrossRef]

45. Kohl, A.; Stammer, D.; Cornuelle, B. Interannual to decadal changes in the ECCO global synthesis. *J. Phys. Oceanogr.* **2007**, *37*, 313–337. [CrossRef]

46. Merrifield, M.A.; Thompson, P.R.; Lander, M. Multidecadal sea level anomalies and trends in the western tropical Pacific. *Geophys. Res. Lett.* **2012**, *39*. [CrossRef]

47. Peng, D.; Palanisamy, H.; Cazenave, A.; Meyssignac, B. Interannual Sea Level Variations in the South China Sea Over 1950–2009. *Mar. Geod.* **2013**, *36*, 164–182. [CrossRef]

48. Strassburg, M.W.; Hamlington, B.D.; Leben, R.R.; Manurung, P.; Lumban Gaol, J.; Nababan, B.; Vignudelli, S.; Kim, K.Y. Sea level trends in Southeast Asian seas. *Clim. Past* **2015**, *11*, 743–750. [CrossRef]

49. Cherniawsky, J.Y.; Foreman, M.G.G.; Kang, S.K.; Scharroo, R.; Eert, A.J. 18.6-year lunar nodal tides from altimeter data. *Cont. Shelf. Res.* **2010**, *30*, 575–587. [CrossRef]

50. Woodworth, P.L. A Note on the Nodal Tide in Sea Level Records. *J. Coast. Res.* **2012**, *28*, 316–323. [CrossRef]